Synthesis and characterization of high surface area molybdenum nitride

R. N. PANDA
Institute of Nanotechnology, Forschungszentrum Karlsruhe, D 76021, Germany

S. KASKEL*
Inorganic Chemistry Department, Technical University of Dresden, Mommsenstr. 6, D-01062 Dresden, Germany
E-mail: stefan.kaskel@chemie.tu-dresden.de

Published online: 3 March 2006

The synthesis of high surface area γ-Mo_2N materials using the nitridation of oxide precursors MoO_3, H_2MoO_5, and $H_2MoO_5{\cdot}H_2O$ with ammonia at 650°C is described. H_2MoO_5 and its hydrated form were obtained from the reaction of MoO_3 and diluted H_2O_2. The materials were characterized by means of X-ray powder diffraction, thermal analysis and nitrogen physisorption. Directly after the preparation, the nitride materials were subjected to different processing conditions: (1) contact to air, (2) inert gas or (3) treated with 1% O_2(g)/N_2(g) gas mixture (Passivation). The synthesis and passivation conditions critically affect the specific surface area of the final product. By means of XRD a minor quantity of MoO_2 was detected in most of the products. The highest specific surface area of the nitrides was 158.4 m^2/g for γ-Mo_2N materials using $H_2MoO_5{\cdot}H_2O$ as the precursor. The high specific surface area corresponds to an average particle diameter of 4 nm, assuming a cubic morphology of the nanocrystals ($d_p = 6/\rho S_{BET}$, $\rho = 9.5$ g/cc). The nitrogen physisorption isotherms of γ-Mo_2N are of type IV, but pore sizes and diameters differ significantly depending on the synthesis conditions due to different defect structures of the intermediates generated in the course of the topotactic transformation of the oxides to nitrides.

1. Introduction

Transition metal carbides and nitrides have received considerable attention in recent years because of their catalytic activity in hydrotreating applications [1–5]. Typically, γ-Mo_2N is synthesized in a temperature programmed reaction from commercial MoO_3 with low specific surface area by heating the powder in ammonia [5–7]. Boudart showed that a topotactic solid state transformation of MoO_3 into γ-Mo_2N is involved and proposed a parallel crystallographic orientation of the $(010)_{MoO3}$ and $(100)_{Mo2N}$ lattice planes [6]. The temperature program plays an important role in controlling the progress of the reaction during the transformation of MoO_3 and is crucial for obtaining high surface area materials. The formation of MoO_2 as a side product has been reported [6, 8]. The presence of MoO_2 hinders the total transformation of the MoO_3 to the γ-Mo_2N phase. For systematic catalytic investigations, the synthesis of materials with high surface area but without impurities is crucial. Various attempts have been made to improve surface area and phase purity at the same time. Li *et al*. have used heteropolyacids as precursors for the nitridation reaction [9, 10]. An efficient method to maximize the specific surface area is the use of oxidic supports such as Al_2O_3 [11–13] and activated carbon [14]. However, for such materials it is difficult to determine the intrinsic activity for the nitride. Wang has used the heptamolybdate, $(NH_4)_6Mo_7O_{24}$, as the precursor for the impregnation of an alumina support and subsequent nitridation with ammonia [15].

Another strategy is to enhance the surface area of the starting material using sol-gel techniques. In the following, we report the fabrication of high surface area γ-Mo_2N materials using sol-gel derived oxide precursors. However, the alkoxides of molybdenum are expensive and not suitable for commercial applications. Instead, we have used a peroxide approach. $H_2MoO_5{\cdot}H_2O$- and H_2MoO_5-gels were prepared from MoO_3 and H_2O_2 and used as

*Author to whom all correspondence should be addressed.
0022-2461
DOI: 10.1007/s10853-006-5112-3

precursors. The results are compared with the corresponding products, obtained using commercial MoO_3 as the solid state precursor.

2. Experimental

2.1. Precursor synthesis

The synthesis of H_2MoO_5 ($MoO_2(OH)(OOH)$) and its hydrated form have been described earlier [16]. MoO_3 (2 g, Aldrich, 99.99%, $S_g = 0.84$ m^2/g) was dissolved in 100 ml of 30% H_2O_2 solution with constant stirring. The solution was filtered in order to remove any precipitates and the filtrate was stored for 24h. Hereafter, the solution was concentrated by evaporation and dried at 90°C for 24h in air. The yellow crystalline products obtained were phase pure H_2MoO_5 as confirmed by X-ray powder diffraction. $H_2MoO_5{\cdot}H_2O$ was obtained in the same way but using 15% H_2O_2 solution.

2.2. Nitridation of the precursors

The nitridation reactions were carried out in a tubular quartz reactor (dimension = 65 cm × 1 cm). The dried H_2MoO_5 and $H_2MoO_5{\cdot}H_2O$ precursors were heat treated in an ammonia gas stream (Messer, UHP). 1 g of the precursor powder supported on a quartz wool plug was placed at the center of a vertically aligned reactor. The NH_3(g) flow rates were maintained at 6l/h. The heating rate was 3 K/min. In order to study the solid state reactivity, the precursors were nitrided at various temperatures ranging from 500°C to 700°C with an annealing phase of 1h at the final nitridation temperature. After completion of the reaction, the samples were cooled in the NH_3(g) flow to room temperature and handled in air, passivated or kept under inert conditions using an argon-filled glove box or vacuum line. The passivation was carried out using diluted oxygen (1% O_2 in N_2).

2.3. Characterization

Powder XRD patterns were recorded on a $\theta/2\theta$-STADI-P diffractometer(Stoe) equipped with a position-sensitive detector (7° opening). Nitrogen physisorption experiments were performed on a Micromeritics ASAP 2000 instrument. The samples were evacuated at 250°C for 2h. Alternatively, single point BET measurements were used for passivated samples. For single point measurements, the samples were activated in the temperature range of 150–200°C in a He/N_2 mixture for 2h. Thermogravimetric (TG) and Differential Thermal Analysis (DTA) measurements were carried out using a Netzsch, STA 449 C Jupiter instrument equipped with a Balzer MS Quadrastar 422 mass spectrometer in air. The heating rate used was 5 $Kmin^{-1}$ from room temperature to 1073K.

3. Results and discussion

3.1. Reactivity, Phase composition and Specific Surface Area

The reactivity of commercial MoO_3, H_2MoO_5 and $H_2MoO_5{\cdot}H_2O$ was compared. The XRD patterns of the peroxo precursors are shown in Fig. 1(a) and (b). The phases were identified as H_2MoO_5 (PDF 41–359) and $H_2MoO_5{\cdot}H_2O$ (PDF 41–60), respectively. Only one weak reflection in the XRD pattern of $H_2MoO_5{\cdot}H_2O$ ($2\theta \approx 11.7°$) could not be indexed. The compounds have a layered structure with an inter-planar spacing between the layers of 6.19 Å [16]. The single point BET surface areas, S_{BET}, of the precursors, i.e. commercial MoO_3, H_2MoO_5 and $H_2MoO_5{\cdot}H_2O$, were found to be 0.84 m^2/g, 4.43 m^2/g and 7.06 m^2/g, respectively. In order to optimize the synthetic parameters for achieving high surface area nitrides, the powders were nitrided at various temperatures ranging from 500°C–700°C.

Using commercial MoO_3 as the precursor, below 600°C, only MoO_2 was obtained as the main product (Fig. 2). At higher temperature, 650°C, γ-Mo_2N was the major phase along with a minor quantity of MoO_2. Pure γ-Mo_2N was obtained when the nitridation temperature was raised to the temperature of 700°C. The cubic γ-Mo_2N (fcc) was identified from the X-ray diffraction patterns (PDF 24–768).

γ-Mo_2N materials synthesized at 650°C have specific surface areas as high as 105 m^2/g. Since the Bragg reflections of the MoO_2 side products have a small half width, the contribution of MoO_2 to the specific surface area must be small.

In order to produce γ-Mo_2N materials with higher surface area and high phase purity, we have performed nitridation experiments on various chemically different

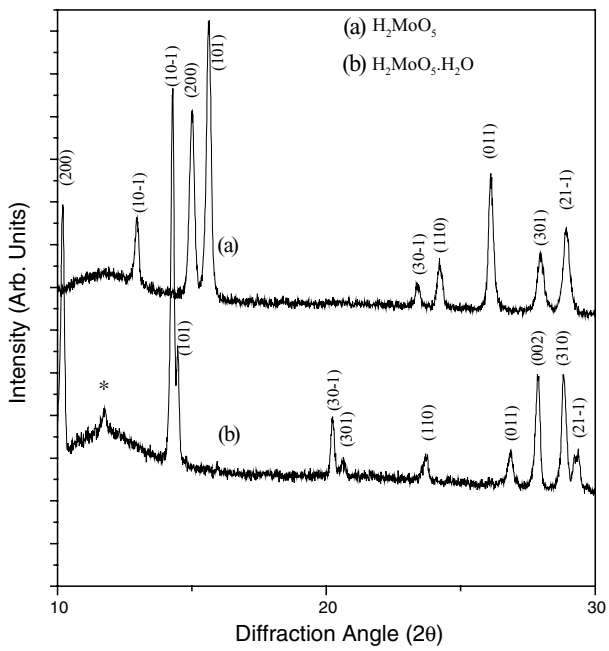

Figure 1 XRD patterns of the peroxo molybdates (a) H_2MoO_5 and (b) $H_2MoO_5{\cdot}H_2O$.

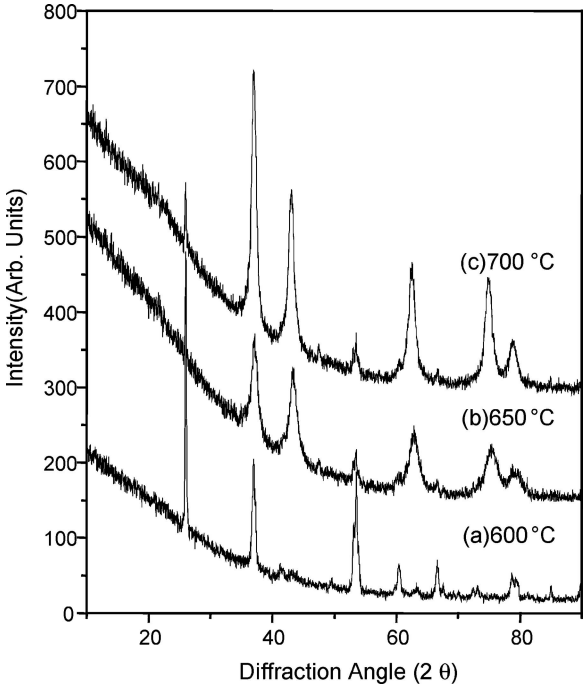

Figure 2 XRD patterns of γ-Mo_2N materials obtained after nitridation of the commercial MoO_3 powders at different temperatures; (a) 600°C, (b) 650°C and (c) 700°C. Samples were handled in inert gas.

precursors such as H_2MoO_5 and $H_2MoO_5 \cdot H_2O$, at 650°C. Fig. 3(a, b and c) depicts the XRD patterns of molybdenum nitrides synthesized by the nitridation of commercial MoO_3, H_2MoO_5 and $H_2MoO_5 \cdot H_2O$ precursors at 650°C using NH_3(g). In the reaction of the H_2MoO_5 precursor at 650°C, a pure product of γ-Mo_2N was obtained with a surface area of 114.6 m^2/g (Table I, Fig. 3). An even higher surface area of 158.5 m^2/g, was observed using

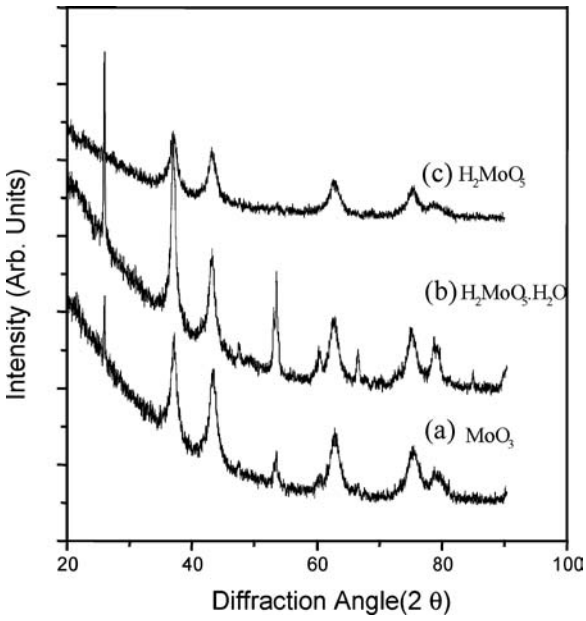

Figure 3 XRD patterns of γ-Mo_2N nitrides synthesized using various precursors at 650°C; (a) Commercial MoO_3, (b) $H_2MoO_5 \cdot H_2O$ and (c) H_2MoO_5.

TABLE I. Experimental parameters and specific surface areas (S_{BET}) of the precursors and γ-Mo_2N materials synthesized at 650°C

Precursor	Aftertreatment	S_{BET}(m^2/g) (Precursor)	S_{BET}(m^2/g) (Nitride)
MoO_3	Glove box	0.84	105.0
$H_2MoO_5 \cdot H_2O$	Glove box	4.43	158.4
H_2MoO_5	Glove box	7.06	124.0
MoO_3	Passivation	0.84	139.0

$H_2MoO_5 \cdot H_2O$ as precursor for the nitridation reaction. Thus, using peroxo precursors, the specific surface area of the nitridation products is significantly higher as compared with commercial MoO_3 powder under similar reaction conditions. However, the XRD patterns also indicate the presence of MoO_2 impurities (Fig. 3b). Pure γ-Mo_2N with lower surface area (S_{BET} = 50 m^2/g) was obtained from $H_2MoO_5 \cdot H_2O$ using the same reaction conditions and passivation with 1%O_2/N_2. In the XRD patterns of the γ-Mo_2N samples synthesized from commercial MoO_3 also some minor quantity of a MoO_2 impurity is detected. The highest specific surface area for a nitride prepared from MoO_3 was 139 m^2/g using the passivation technique.

Significant differences were observed for the (111) and (200) reflections of the cubic γ-Mo_2N. Typically, materials with a higher I_{200}/I_{111} ratio close to 1.0 have higher specific surface areas than those with I_{200}/I_{111} less than 0.6. Fig. 4 shows the correlation of S_{BET} and I_{200}/I_{111} for the γ-Mo_2N materials synthesized from commercial MoO_3 at the nitridation temperature of 650°C.

Depending on the precursor, temperature program, and aftertreatment the materials may also differ in nitrogen content due to the presence of the surface oxide layers. The nitrogen content was indirectly analyzed using thermogravimetry (Fig. 5). The oxidation of γ-Mo_2N nitride materials synthesized from H_2MoO_5 precursors starts at 100°C, whereas materials obtained from commercial MoO_3 powder show a weight gain only above 270°C. This difference can be attributed to the difference in the values of the surface areas obtained for γ-Mo_2N nitrides synthesized at 650°C and 700°C (86 m^2/g using H_2MoO_5

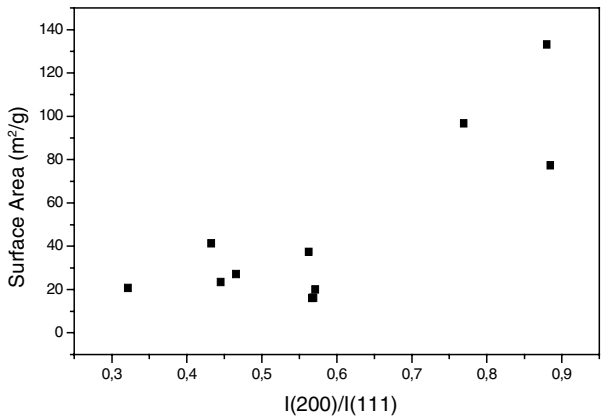

Figure 4 Correlation of S_{BET} and I_{200}/I_{111} for passivated samples of γ-Mo_2N synthesized at 650°C from MoO_3.

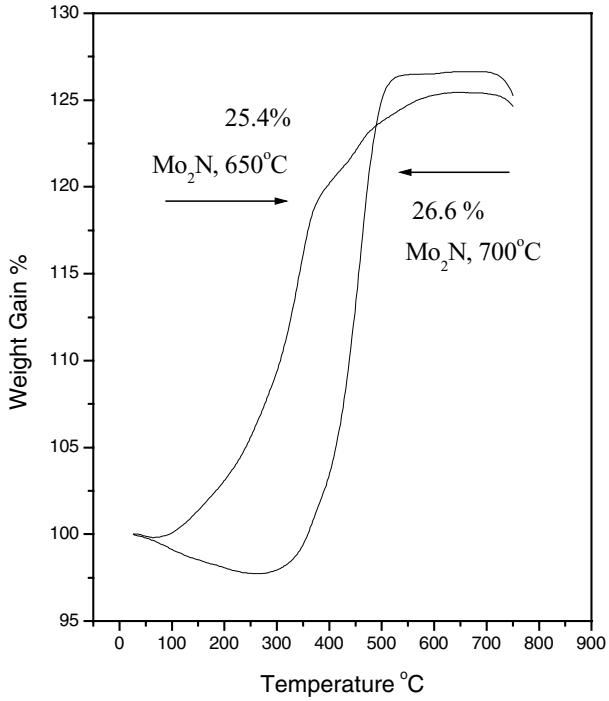

Figure 5 Thermal analyses of γ-Mo_2N materials synthesized from MoO_3 at (a) 650°C and (b) 700°C (duration of 1h).

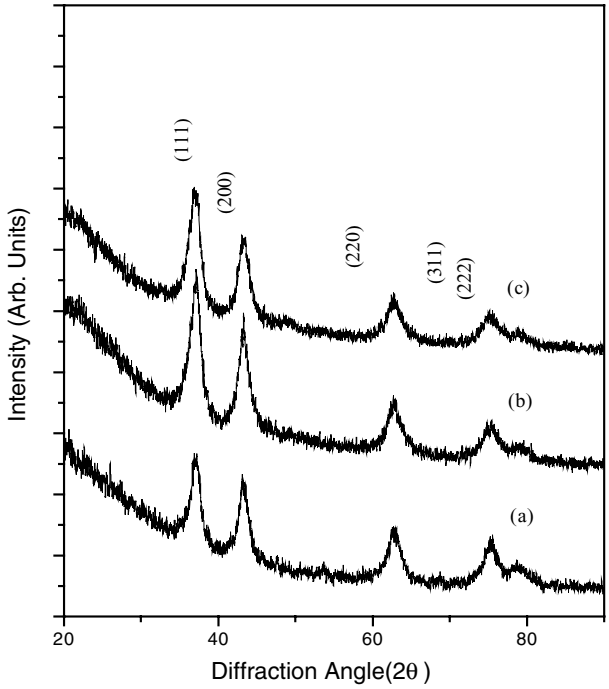

Figure 6 XRD patterns of γ-Mo_2N materials synthesized from H_2MoO_5 precursors at 650°C; (a) treated in inert gas, (b) air exposed and (c) passivated with $1\%O_2/N_2$ mixture.

and 24 m^2/g using commercial MoO_3 precursors). The observed weight gain is 25.4% and 26.6%, for the samples synthesized at 650°C and 700°C, respectively and considerably lower as compared to the expected value of 40% for the oxidation of Mo_2N to MoO_3. This difference is probably due to significant amounts of oxides on the outer surface of the nitride nanoparticles and oxynitride formation.

XRD patterns of γ-Mo_2N materials synthesized from H_2MoO_5 precursors at 650°C, subjected to different treatments after sample preparation, are shown in Fig. 6(a), (b) and (c). γ-Mo_2N materials synthesized from H_2MoO_5 precursors were subjected to the following treatments: (1) samples were handled in Argon, (2) samples were exposed to air and (3) samples were passivated with $1\%O_2/N_2$ gas mixture. The XRD patterns do not show significant differences. The intensity ratios, I_{200}/I_{111} for the samples were 0.76, 0.78, and 0.8 respectively. Although, the intensity ratios are almost identical, differences in the specific surface area were detected. Thus, the sample handled in Argon had a surface area of 114 m^2/g whereas the passivated sample had a reduced surface area of 86 m^2/g. Obviously, the passivation and oxidation during the aftertreatment significantly affects the morpholgical properties.

In order to explain the differences in surface area and reactivity depending on the precursor, the thermal decomposition of $H_2MoO_5{\cdot}H_2O$ and H_2MoO_5 precursors was studied in air atmosphere by means of TG and DTA (Fig. 7 and 8). The $H_2MoO_5{\cdot}H_2O$ precursor shows two exothermic peaks at 70°C and 218°C. The first peak indicates the removal of structural H_2O whereas the

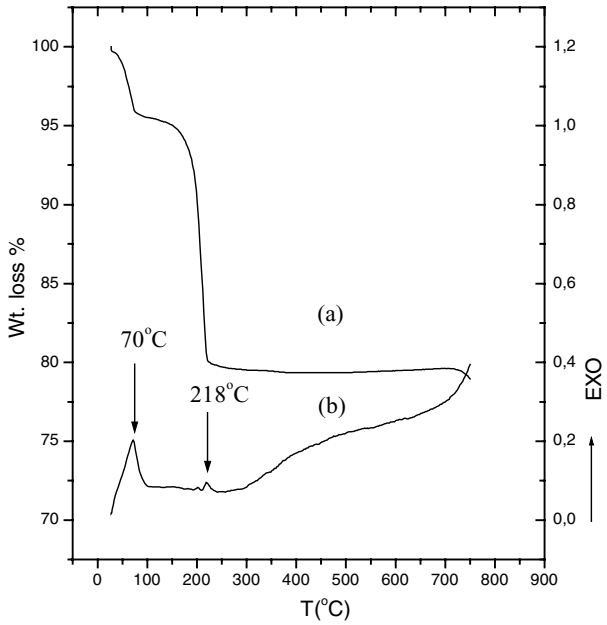

Figure 7 TG (a) and DTA (b) of the $H_2MoO_5{\cdot}H_2O$ precursor.

second peak corresponds to the thermal decomposition of the H_2MoO_5 intermediates to MoO_3. However, the observed weight loss is only 16% and thus lower than the calculated loss of 19.1% for the thermal decomposition of $H_2MoO_5{\cdot}H_2O$ indicating the formation of oxygen deficient molybdenum oxide, $MoO_{3-\delta}$ during the decomposition of $H_2MoO_5{\cdot}H_2O$ precursors. For H_2MoO_5 (Fig. 8) an endothermic peak is observed at

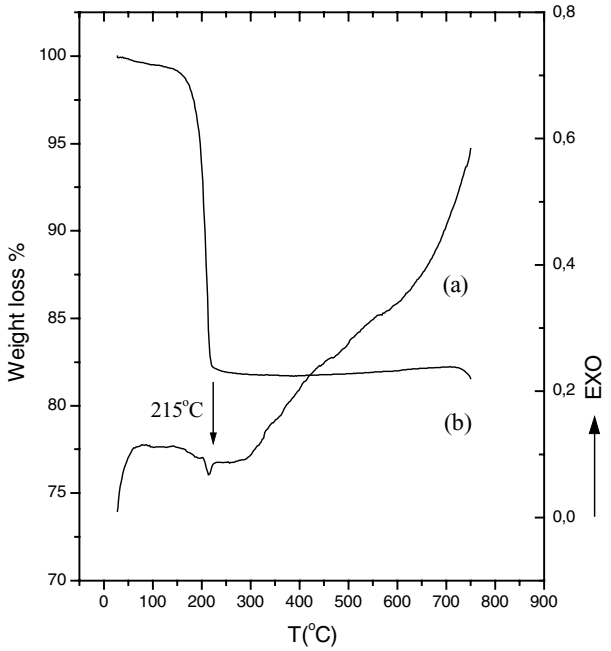

Figure 8 DTA (a) and TG (b) of the H_2MoO_5 precursor.

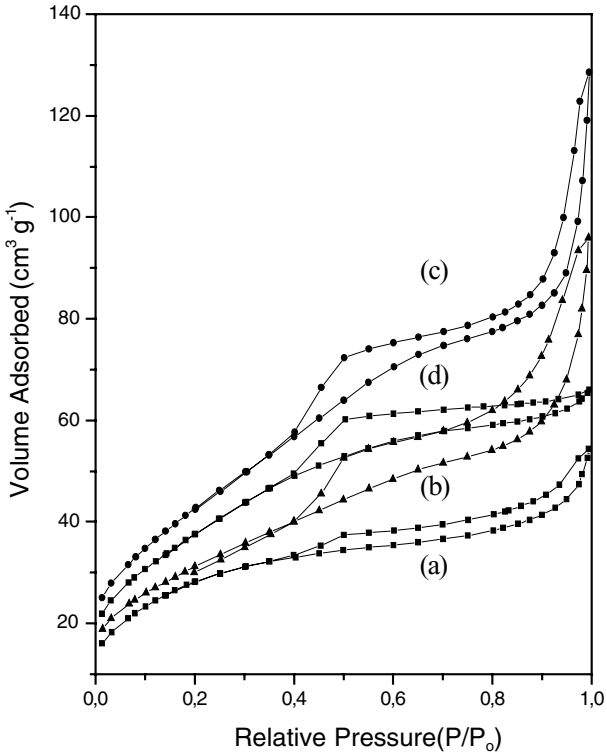

Figure 9 Nitrogen physisorption isotherms of γ-Mo_2N samples synthesized at 650°C using different precursors; (a) Commercial MoO_3, (b) $H_2MoO_5{\cdot}H_2O$, (c) H_2MoO_5 and (d) MoO_3 (passivated).

215°C and the corresponding weight loss was found to be 17.6% which was higher than the value obtained from the thermal decomposition of $H_2MoO_5{\cdot}H_2O$. Thus, the thermal decomposition products of $H_2MoO_5{\cdot}H_2O$ and H_2MoO_5 slightly differ in composition. The differences in the decomposition are crucial for the development of the nitride microstructure. However, it is unknown if the intermediates observed within the course of the peroxide decomposition are also relevant in ammonia atmosphere. In principle, ammonia could also lead to the formation of ammonium salts as intermediates. However, since the decomposition into the oxide is observed at temperatures below 300°C and the oxygen substitution takes place only above 500°C, the oxides $MoO_{3-\delta}$ are probably the relevant intermediates. XRD analyses of the thermal decomposition products of H_2MoO_5 in NH_3(g) atmosphere at 300°C show two peaks of low intensity ($2\theta = 22.3$ and 26.1°) and may be attributed to Mo_8O_{23} (PDF 74–1661).

3.2. Physisorption isotherms and porosity

Physisorption isotherms not only provide information on the total specific surface area but also allow to detect pores that are formed in between particles and thus give valuable information on the morphology of the constituting nanoparticles [17]. Fig. 9 shows the nitrogen adsorption and desorption isotherms of γ-Mo_2N samples obtained at 77 K synthesized at 650°C using various precursors (MoO_3, $H_2MoO_5{\cdot}H_2O$, and H_2MoO_5). All isotherms are of type IV indicating the presence of interparticle mesopores. Depending on the precursor, significant differences in the hysteresis shape are observed. The nitride obtained from MoO_3 has an H_4 type hysteresis due to the presence of plate-like particles, whereas the other materials show more or less an H_2 hysteresis which indicates a wide distribution of pore sizes in the mesopore range. In addition, the peroxo precursor-derived Mo_2N materials show the presence of some macropores. Thus, the precursor chemistry can be used to affect the morphology of the final product in the oxide to nitride transformation. However, passivation or aftertreatment equally affects surface area and pore morphology (Fig. 9). The highest BET surface area of 158.4 m^2/g was observed using $H_2MoO_5{\cdot}H_2O$ precursors. This value corresponds to an average particle size of 4 nm, assuming spherical or cubic morphology and a density of $\rho = 9.5$ g/cc for γ-Mo_2N.

4. Conclusion

High surface area γ-Mo_2N nitride materials were synthesized using three different precursors: commercial MoO_3, H_2MoO_5 and $H_2MoO_5{\cdot}H_2O$ with different specific surface areas, decomposition behavior and reactivity. Phase composition and specific surface area depend on the precursor but also on the aftertreatment. High surface area Mo_2N is air sensitive and sometimes pyrophoric. Thus, air exposed samples typically have low surface areas (30–50 m^2/g) and show significant amounts of oxide impurities such as MoO_2. Thermogravimetric analyses also indicate significant amounts of oxidic im-

purities. The nitrides characterized using consequent handling under inert conditions show lower amounts of oxide impurities and higher specific surface areas up to 158 m^2/g. The precursor significantly affects the morphology and surface area of the final product. The latter is attributed to differences in the thermal decomposition pathway and the microstructure of the starting material.

Acknowledgment

This research project was supported by the German Research Foundation (DFG, contract number: KA 1698/1–1).

References

1. E. FURIMSKY, *Appl. Catal. A* **240** (2003) 1.
2. S. RAMANATHAN and S. T. OYAMA, *J. Phys. Chem.* **99** (1995) 16365.
3. E. J. MARKEL and J. W. VANZEE, *J. Catal.* **126** (1990) 643.
4. H. ABE, T. K. CHEUNG and A. T. BELL, *Catal. Lett.* **21** (1993) 11.
5. J. G. CHOI, J. R. BRENNER, C. W. COLLING, B. G. DEMCZYK, J. L. DUNNING and L. T. THOMPSON, *Catal. Today.* **15** (1992) 201.
6. L. VOLPE and M. BOUDART, *J. Solid State Chem.* **59** (1985) 332.
7. S. T. OYAMA, *Catal. Today.* **15** (1992) 179.
8. A. GUERRERO-RUIZ, Q. XIN, Y. J. ZHANG, A. MAROTO-VALIENTE and I. RODRIGUEZ-RAMOS, *Langmuir.* **15** (1999) 4927.
9. S. Z. LI and J. S. LEE, *J. Catal.* **178** (1998) 119.
10. S. Z. LI and J. S. LEE, *J. Catal.* **173** (1998) 134.
11. T. MIYAO, K. OSHIKAWA, S. OMI and M. NAGAI, *Stud. Surf. Sci. Catal.* **106** (1997) 255.
12. M. NAGAI, Y. GOTO, O. UCHINO and S. OMI, *Catal. Today.* **45** (1998) 335.
13. H. K. PARK, J. K. LEE, J. K. YOO, E. S. KO, D. S. KIM and K. L. KIM, *Appl. Catal. A* **150** (1997) 21.
14. J. TRAWCZYNSKI, *Catal. Today.* **65** (2001) 343.
15. S. T. WANG, X. WANG, Z. D. ZHANG and Y. T. QIAN, *J. Mater. Sci.* **38** (2003) 3473.
16. Y. KURUSU, *Bull. Chem. Soc. Jpn.* **54** (1981) 293.
17. F. ROUQUEROL, J. ROUQUEROL and K. SING, *Adsorption by Powders and Porous Solids*, Academic Press, London, (1999).

Received 3 May 2004
and accepted 7 July 2005